Three-level NPC Converter-based Neuronal Direct Active and Reactive Power Control of the Doubly fed Induction Machine for Wind Energy Generation

Sarra Massoum[1], Abdelkader Meroufel [1], Brahim Elkhalil Youcefa[1], Ahmed Massoum[1], Patrice Wira [2]

1- Department of Electrical Engineering, Djillali Liabes University, Sidi Bel Abbes, Algeria
lalem_sarra@yahoo.fr (Corresponding authors), meroufelaek@yahoo.fr, ahmassoum@yahoo.fr, elyoucbar@yahoo.fr

2- Haute Alsace University, 68093 Mulhouse France
patrice.wira@uha.fr

ABSTRACT
In this paper, neuronal direct power control (DPC) strategy is applied for a doubly fed induction generator (DFIG) based wind energy generation system. Used in three level neutral point clamped (NPC) rectifiers, to directly control the active and reactive power, switching vectors for rotor side converter were selected from the optimal switching table using the estimated stator flux position and the errors of the active and reactive power, also the grid side is controlled by direct power control based a grid voltage position to ensure a constant DC- link voltage. This approach is validated by using MATLAB/SIMULINK software and simulation results can prove the excellent performance of this control as improving power quality and stability of wind turbine.

Keywords: Neuronal Direct power control (DPC), Doubly fed induction generator (DFIG), Three level neutral point clamped (NPC), Active power, Reactive power, DC-link, Wind turbine.

1. INTRODUCTION

In recent years, the majority of electricity has been generated from traditional fossil sources, such as charcoal and oil and gas energy, which are nonrenewable sources. A great emissions of carbon dioxide has been emitted to the atmosphere, that is a result of serious warming of the global. For this reason and due to the modern development of electricity and production technologies, this last has been replaced by a new technology that is superseding old fuel burner power generation units. Among these recent electricity generation technologies, the renewable energy converters are magnificently shining with respect to their smaller size, lower cost per unit and being more environmental friendly [1].

There were several types of generators that have been used as wind energy converters. Induction generators of different kinds have become more accepted in wind energy conversion field [2]. Induction generators, especially doubly fed induction generators are becoming more and more popular in renewable source employment [3].

The wind energy is the most important potential, the power of wind turbines energy installed on the world is growing every year. Nowadays, variable speed wind turbine energy system is based on the doubly fed induction generator (DFIG) which is mostly used in wind turbine, the principal advantage of this machine is to have a three phase static converters sized for a part of the nominal power of the (DFIG), that makes a significant economic benefits compared to other possible solutions of electromechanical conversion.

The major components of a typical wind energy conversion system include a wind turbine, a generator, an interconnection apparatus and a control system. Wind turbines convert the kinetic energy from the wind into electricity that can be fed to the grid for distribution. As shown in the Figure 1, the power originates from the mass flow of moving air. Aero-dynamical forces rotate the blade to transform the wind energy to mechanical energy. Then, the wind turbine shaft transports the energy to the generator, which is connected to the grid. To improve the quality of electrical power supplied to the grid, speed and control mechanisms are employed [4].

The doubly fed induction generator is one of the generation systems, commercially available in the wind energy market, which its stator winding is directly connected to the grid and its rotor winding is connected to the grid through a frequency converter as shown in

Figure 1, along with operation and four quadrant active and reactive powers [5].

Based on the principles of DTC for electrical machine drives, direct power control (DPC) for three-phase PWM rectifiers was proposed in [6], [7]. In [6], an optimal switching table is used to deliver an optimal vectors control for the converter that is based on the active and reactive powers error between the reference and estimated values of active and reactive powers and the angular position of the estimated converter terminal voltage vector. The converter terminal voltage was estimated using the dc link voltage and converter switching states.

In this paper, a neuronal direct power control (NDPC) strategy is proposed for NPC three-level rectifiers based on wind energy generation system in order to control the active and reactive power. The NDPC is applied for both stator and rotor power converters, the stator active and reactive power is controlled by rotor side converter when the DC link voltage is maintained constant using the grid side converter.
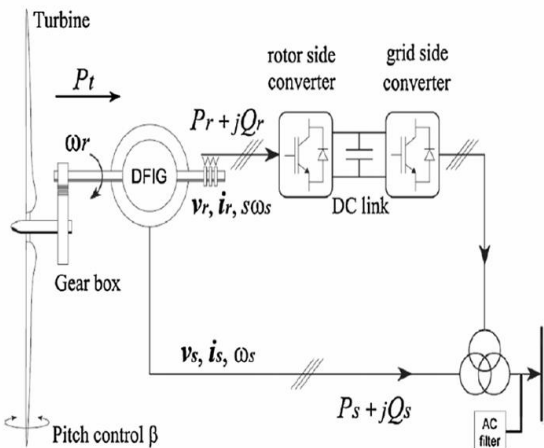

Fig. 1. Schematic diagram of DFIG-based wind generation system.

2. MODELING AND CONTROL OF THE WIND SYSTEM

The general electrical state model of the induction machine obtained using Park transformation is given by:

$$
\begin{aligned}
V_{sd} &= R_s I_{sd} + \frac{d\phi_{sd}}{dt} - \omega_s \phi_{sq} \\
V_{sq} &= R_s I_{sq} + \frac{d\phi_{sq}}{dt} + \omega_s \phi_{sd} \\
V_{rd} &= R_r I_{rd} + \frac{d\phi_{rd}}{dt} - \omega_r \phi_{rq} \\
V_{rq} &= R_r I_{rq} + \frac{d\phi_{rq}}{dt} + \omega_r \phi_{rd}
\end{aligned}
\tag{1}
$$

$$
\begin{aligned}
\phi_{sd} &= L_s I_{sd} + L_m I_{rd} \\
\phi_{sq} &= L_s I_{sq} + L_m I_{rq} \\
\phi_{rd} &= L_r I_{rd} + L_m I_{sd} \\
\phi_{rq} &= L_r I_{rq} + L_m I_{sq}
\end{aligned}
\tag{2}
$$

Electromagnetic torque equation is given by:

$$
T_{em} = \frac{P L_m}{L_s}\left(\phi_{sd} I_{rq} - \phi_{sq} I_{rd}\right)
\tag{3}
$$

And its associated motion equation is given by:

$$
T_{em} - T_r = J \frac{d\Omega}{dt}
\tag{4}
$$

Stator active and reactive powers are expressed by:

$$
\begin{aligned}
P_s &= 3/2\left(V_{sd} I_{sd} + V_{sq} I_{sq}\right) \\
Q_s &= 3/2\left(V_{sq} I_{sd} - V_{sd} I_{sq}\right)
\end{aligned}
\tag{5}
$$

In the state space representation, the system is given as:

$$
[\dot{X}] = [A][X] + [B][U]
\tag{6}
$$

With:

$$
[X] = [\phi_{sd}\,\phi_{sq}\,I_{rd}\,I_{rq}]^T ; [U] = [V_{sd}\,V_{sq}\,V_{rd}\,V_{rq}]^T
$$

Where:

$$
[A] = \begin{bmatrix}
\dfrac{-1}{T_s} & \omega_s & \dfrac{L_m}{T_s} & 0 \\[2mm]
-\omega_s & \dfrac{-1}{T_s} & 0 & \dfrac{L_m}{T_s} \\[2mm]
\alpha & -\beta\omega_e & -\delta & \omega_r \\[2mm]
\beta\omega_e & \alpha & -\omega_r & -\delta
\end{bmatrix}
$$

$$
[B] = \begin{bmatrix}
1 & 0 & 0 & 0 \\[2mm]
0 & 1 & 0 & 0 \\[2mm]
\dfrac{-L_m}{\sigma L_s L_r} & 0 & \dfrac{1}{\sigma L_r} & 0 \\[2mm]
0 & \dfrac{-L_m}{\sigma L_s L_r} & 0 & \dfrac{1}{\sigma L_r}
\end{bmatrix}
$$

α, β And δ are constants defined as follows:

$$
\alpha = \frac{L_m}{\sigma T_s L_s L_r} ; \ \beta = \frac{L_m}{\sigma L_s L_r} ; \ \beta = \frac{1}{\sigma}\left(\frac{1}{T_r} + \frac{L_m^2}{T_s L_s L_r}\right);
$$

$$
\omega_e = \omega_s - \omega_r
$$

3. CONTROL OF GENERATOR AND ITS ASSOCIATED CONVERTERS

Figure 2 demonstrates the main circuit topology of a DFIG system with the three level neutral point clamped (NPC) rectifiers, which is composed of a grid side converter (GSC), a rotor side converter (RSC) and a DC-link voltage capacitor.

Fig. 2. Circuit topology of the three level neutral point clamped (NPC) rectifiers for DFIG.

3.1. Three level NPC inverter topology and modeling

The converter used in this project is a Neutral-Point-Clamped (NPC) three-level converter with three bridge legs. "Three-level" means that each bridge leg, A, B and C can have three different voltage states. The converter topology can be seen in Figure 3. Switch 1 and 3 on each leg are complementary, which means that when switch 1 is on, switch 3 is off and vice versa. Switch 2 and 4 is the other complementary switching pair [8].

Fig.3. The main circuit topology of the three level neutral point- clamped.

If each of the capacitors has a constant voltage of $0.5\ U_{dc}$, then having the two upper switches on will give an output voltage of U_{dc} compared to level 0, switch 2 and 3 on will give $0.5\ U_{dc}$ and by having the two lower switches on, an output voltage of 0 will occur. In addition to these three states there is a forbidden state where the first switch is on while the second is off [8].

Table 1. The bridge leg voltages at different combinations of switch states.

Leg state	U_{a0}	S_{1U}	S_{2U}	S_{3U}	S_{4U}
2	U_{dc}	ON	ON	OFF	OFF
1	$0.5\ U_{dc}$	OFF	ON	ON	OFF
0	0	OFF	OFF	ON	ON

Three-level diode-clamped inverter, which is also known as a neutral-point clamped (NPC) inverter is used. In the Figure 3, the DC-link capacitor has been split to create the neutral point O. An additional clamping diode is connected in series with a pair of devices with bypass diode between the neutral point and the center of the pair, as shown. All three phase groups are identical. The phase U, for example, gets the state P (positive bus voltage) when the switches S_{1U} and S_{2U} are closed, whereas it gets the state N (negative bus voltage) when S_{3U} and S_{4U} are closed. At neutral-point clamping, the phase gets the O state when either S_{2U} or S_{3U} conducts depending on positive or negative phase current polarity, respectively. For balancing neutral-point voltage, the average current injected at O should be zero [9].

Fig. 4. Vectors and sector division of DPC system in three-level NPC rectifier

4. DIRECT ACTIVE AND REACTIVE POWER CONTROL PRINCIPLE

The dynamic behavior of a DFIG is described according to (1) and (2) of the general electrical state model written in the term of space vectors in a rotor reference frame, the stator active and reactive power inputs from the network can be calculated as:

$$P_s = -\frac{3}{2}\frac{L_m}{\sigma L_s L_r}\omega_s|\phi_s\|\phi_r|\sin\theta \qquad (7)$$

$$Q_s = \frac{3}{2}\frac{L_m}{\sigma L_s L_r}\omega_s|\phi_s|\left(|\phi_r|\cos\theta - \frac{L_r}{L_m}|\phi_s|\right) \qquad (8)$$

Where $\sigma = \left(1 - L_m^2/L_s L_r\right)$, ω_s and θ are the synchronous angular frequency and angle between the rotor and stator flux linkage vectors.

The fact that the stator is directly connected to the grid provides a stator flux vector with constant amplitude and a constant $\omega_s - \omega_r$ in the rotor reference frame. Derivation along (7) and (8) results in the following equations:

$$\frac{dP_s}{dt} = -\frac{3}{2}\frac{L_m}{\sigma L_s L_r}\omega_s|\phi_s|\frac{d(|\theta_r|\sin\theta)}{dt} \qquad (9)$$

$$\frac{dQ_s}{dt} = \frac{3}{2}\frac{L_m}{\sigma L_s L_r}\omega_s|\phi_s|\frac{d(|\phi_r|\cos\theta)}{dt} \qquad (10)$$

Neglecting the rotor resistance in (11), we have:

$$V_r = R_r I_r + \frac{d\Psi_r}{dt} \qquad (11)$$

The rotor flux variations in the rotor reference frame are approximated as:

$$\frac{d\Psi_r}{dt} = V_r \qquad (12)$$

According to (12) the rotor flux moves in the direction of the applied rotor voltage vector and its speed is proportional to the amplitude of the voltage vector.

4.1. DTC Principle

The basic principle of the Direct Power Control (DPC) was proposed by Noguchi [10] and is based on the well-known Direct Torque Control (DTC) for induction machines. In the direct power control, the torque and flux amplitude is replaced by active and reactive powers, the basic concept of this method is using an optimal vectors table to stratify and optimal vectors were being based on the reactive and active powers error, as illustrated in Figure 5 to correctly estimate power and reduce the numbers of implemented voltage sensors, Noguchi proposes the voltage vector estimation. The computation of the time derivative of the measured currents is involved by the implementation of such approach. The noise can be

increased by using the derivative in the control loop, thus increasing the level of distortion.

4.2. Vector and switching states selection in traditional there-level DPC Strategy

The vectors and sector division of DPC strategy are shown in the Figure 4. It divides the vector diagram in twelve sectors which are $\theta_1...\theta_{12}$, in this diagram each sector has one zero vector which is (V_0), one larger vectors are $(V_{Li}, i = 1....6)$, one middle vectors are $(V_{Mi}, i = 1....6)$, and one also small vectors are $(V_{Si}, i = 1....6)$, The magnitude of large vector is $\sqrt{2/3}U_{dc}$, the magnitude of middle vector is $\sqrt{1/2}U_{dc}$ and the magnitude of small vector is $\sqrt{1/6}U_{dc}$.
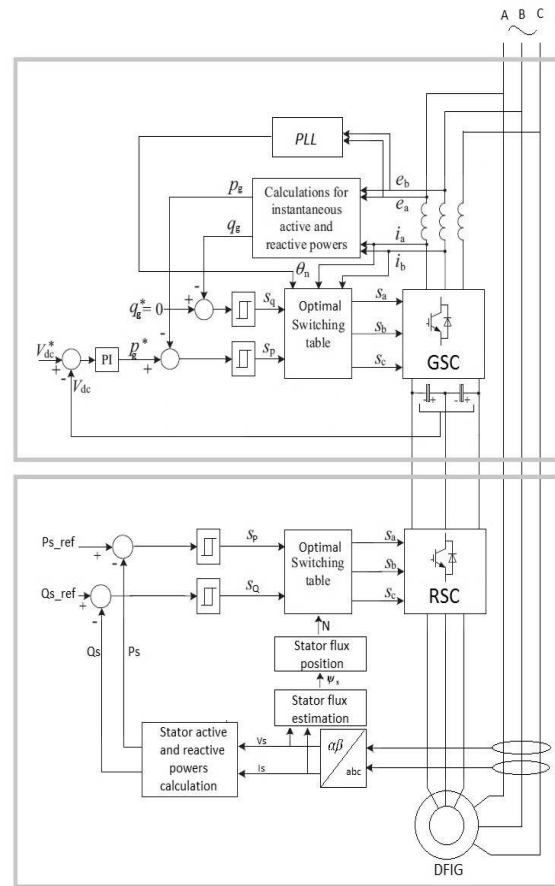

Fig.5. Schematic diagram of classical DPC of DFIG.

4.2. Principle for vector and switching states selection traditional three-level DPC strategy

Figure 5 shows the block scheme of traditional DPC with switching table used in three-level NPC rectifiers. The grid voltage (u_a, u_b, u_c) and currents (i_a, i_b, i_c) are measured to calculate the active and reactive

powers and they are estimated using equations (13) and (14). From equation (15), stator flux angle is calculated and transformed into rotor frame [11].

The active power reference p_g^* ,(delivered from the outer DC voltage closed loop PI controller) and the reactive power reference q_g^* are compared with active power p_g and reactive power q_g respectively. Then the errors are processed of S_p and S_q which may become 1 (means instantaneous power needs to be increased) or 0 (means instantaneous power needs to be decreased) as shown in equation below (16). Thus, the most appropriate vector will be selected according to the location of reference vector (θ_n). In other words, a set of certain parameter (S_p, S_q and θ_n) corresponds to a certain optimal vector, and together they constitute the switching state table which is the key technology of three-level DPC strategy [14].

$$P_s = \frac{3}{2}\left(V_{s\alpha}I_{s\alpha} + V_{s\beta}I_{s\beta}\right) \tag{13}$$

$$Q_s = \frac{3}{2}\left(V_{s\beta}I_{s\alpha} + V_{s\alpha}I_{s\beta}\right) \tag{14}$$

$$\phi_s = \int_0^t \left(V_s - R_s I_s\right)dt, \angle\phi_s = \tan g^{-1}\left(\frac{\phi_\beta}{\phi_\alpha}\right) \tag{15}$$

The switching states in the table 2 will optimize the final output performance from two aspects:

Firstly, the switching state should balance the neutral point voltage otherwise the three-level NPC converter will be unable to work normally.

Secondly, the total switching losses of the system should be as small as possible in order to improve efficiency [12].

$$S_z = \begin{cases} 1 \, if z^* - z = \Delta z > H_z \\ 0 \, if z^* - z < -H_z (z = p, q) \end{cases} \tag{16}$$

Two three-level hysteresis comparators are used to generate the respective active and reactive power states S_p and S_q as in Figure 6 shows.
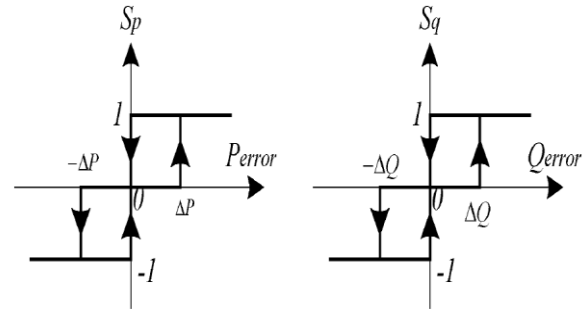

Fig. 6. Active and reactive power compensator.

Table 2. Bridge leg voltages at different combinations of switch states.

S_p	S_q	θ_1	θ_2	θ_3	θ_4	θ_5	θ_6
1	0	V_{S1}	V_{S1}	V_{S2}	V_{S2}	V_{S3}	V_{S3}
1	1	V_{S2}	V_{S2}	V_{S3}	V_{S3}	V_{S4}	V_{S4}
0	0	V_{L1}	V_{M1}	V_{L2}	V_{M2}	V_{L3}	V_{M3}
0	1	V_{M1}	V_{L2}	V_{M2}	V_{L3}	V_{M3}	V_{L4}
S_p	S_q	θ_7	θ_8	θ_9	θ_{10}	θ_{11}	θ_{12}
1	0	V_{S4}	V_{S4}	V_{S5}	V_{S5}	V_{S6}	V_{S6}
1	1	V_{S5}	V_{S5}	V_{S6}	V_{S6}	V_{S1}	V_{S1}
0	0	V_{L4}	V_{M4}	V_{L5}	V_{M5}	V_{L6}	V_{M6}
0	1	V_{M4}	V_{L5}	V_{M5}	V_{L6}	V_{M6}	V_{L1}

5. PHASE-LOCKED-LOOP (PLL)

When dealing with the control of grid connected converters, an aspect that needs to be taken into account is the correct generation of the reference signals, which is obtained with a fast and accurate detection of the phase angle and the grid frequency and voltage. One of the methods to synchronize the reference current of the inverter with the grid voltage is an algorithm called Phase-Locked-Loop (PLL) [13].

The block diagram of the PLL algorithm implemented in the synchronous reference frame is shown in Figure 7.
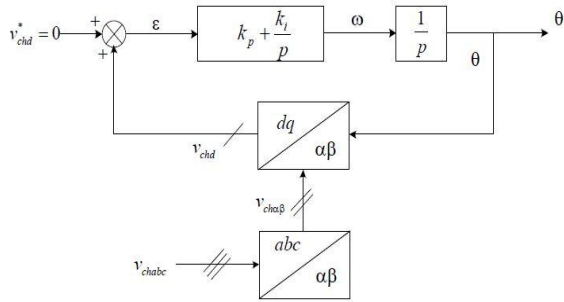
Fig.7.Phase looked loop diagram**.**

The adjustment diagram of the angular positon is given in the figure below:
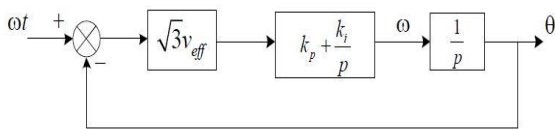

Fig.8. The adjustment diagram of the angular.

$$G(p) = \frac{\sqrt{3}v_{eff}(k_p p + k_i)}{p^2 + \sqrt{3}v_{eff}k_p p + \sqrt{3}v_{eff}k_i} \qquad (17)$$

An identification with a second order transfer function system, the gains of the regulator is given as:

$$k_p = \frac{2\xi\omega_c}{\sqrt{3}v_{eff}} ; k_{i=} \frac{\omega_c^2}{\sqrt{3}v_{eff}}$$

6. ARTIFICIAL NEURAL NETWORK BASED VOLTAGE VECTOR SELECTION

ANN has a very significant role in the field of artificial intelligence. The artificial neurons learn from the data fed to them and keep on decreasing the error during training time and once trained properly, the results are very much same to the results required from them, thus referred to as universal approximators [14].

The most popular neural network used by researchers are the multilayer feed forward neural network trained by the back propagation algorithm. There are different kinds of neural networks classified according to operations they perform or the way of interconnection of neurons. Some approaches use neural networks for parameters estimation of electrical machines in feedback control of their speeds. Here we have used a feed forward neural network to select the voltage vector which replaces the lookup table in the case of C-DTC strategy [15], [16].

In the case presented in this paper the DTC control strategy shown on Table 1 has been implemented.

Neural network has been devised having as inputs: the torque error, the rotor flux error and the position of the flux sector, and as output: the rotor voltage space vector to be generate by the inverter [17], [18].

The network taken in this study is a feed-forward network with first layer of log sigmoid transfer function, second layer of hyperbolic tangent sigmoid transfer function and third layer of linear transfer function. Training method used was again back-propagation. The back-propagation algorithm is used to train the neural networks. As soon as the training procedure is over, the neural network gives almost the same output pattern for the same or nearby values of input. This tendency of the neural networks which approximate the output for new input data is the reason for which they are used as intelligent systems. In matlab command we generate the simulink block ann of switching table by "gensim(net35)" given this model shown in figure 9.
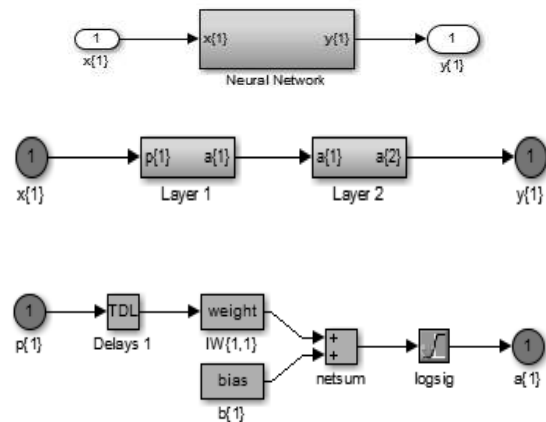

Fig.9. Active and reactive power compensator.

6. SIMULATION RESULTS

Simulation results, given in figures below show the performances of three-level NPC converter-based on neuronal direct active and reactive power control to a wind turbine system. It shows clearly good tracking capabilities of the reference set point for both active and reactive powers.
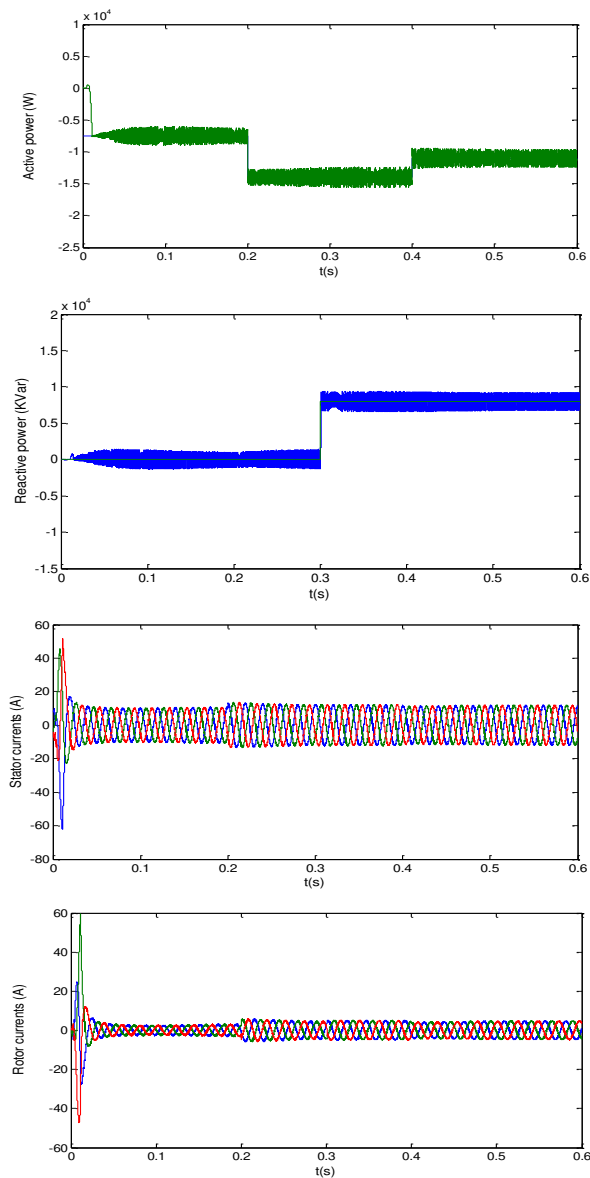
The simulation results of the direct active and reactive power control of the DFIG are shown in the figures below. The simulation is performed using MATLAB/SIMULINK software

Figure 10 shows the active and reactive power transited to the grid with their references and the three phase rotor and stator currents. The responses of both active and reactive power during step change of their references are within a few milliseconds, there is no over shoot of the stator active and reactive power.

Figure 11 shows the electromagnetic and the rotor currents in the reference frame, we can observe that changing the two rotor currents are affected by changing the active and reactive powers.

For the DC link voltage regulation, we observe that the measured DC voltage follows its reference very well.

Simulation results, given in Figures below show the performances of Three-Level NPC Converter-Based Direct Active and Reactive Power Control to a wind turbine system. It shows clearly good tracking capabilities of the reference set point for both active and reactive powers.

Fig.10. Simulation results of the three level NPC converter-based direct power control of the doubly fed induction generator**.**
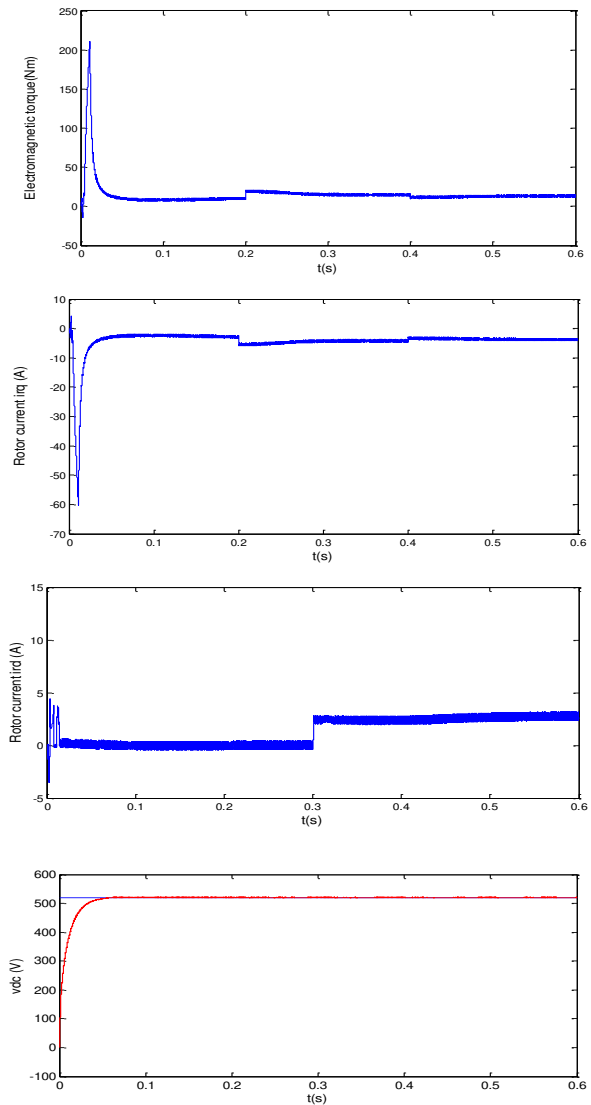

Fig.11. Simulation results of the three level NPC converter-based direct power control of the doubly fed induction generator.

6. CONCLUSION

A direct active and reactive power control method is used in three levels neutral point clamped (NPC) converter and rectifier for a doubly fed induction generator (DFIG) system has been proposed in this paper. The DPC method uses an optimal switching table to stratify an optimal vectors based on the active and reactive flux position. An optimal switching table is performed to select the voltage vectors, this technique has been used for a good tracking of active and reactive power references, with decoupling of these two powers exchanged between the grid and the doubly fed induction generator by controlling the rotor side converter. Simulation results confirm the effectiveness and robustness of the proposed DPC strategy control. The active and reactive powers are decoupled and track their references values very well. Also the DC link voltage is maintained in a constant value.

REFERENCES

[1]. RC. Sonderegger, D. Henderson, S. Bubb, J. Steury. **"Distributed asset insight",** *IEEE Power and Energy Magazine,* Vol. 3,1, pp. 32 - 39, 2004

[2]. R.C. Bansal, T.S. Bhatti, D.P. Kothari, **"Bibliography on the application of induction generators in non-conventional energy systems",** *IEEE Transactions on Energy Conversion,* Vol. 18 3, pp. 433–439, 2003

[3]. R.C. Bansal, **"Three-phase self-excited induction generators: an over view",** *IEEE Transactions on Energy Conversion*, Vol. 20, 2, pp. 292–2999, 2005

[4]. K. Gogas, **"Design of a robust speed and position sensorless decoupled p-q controlled doubly-fed induction generator for variable-speed wind energy applications",** *B. Eng. Concordia University,* Canada, February 2007

[5]. M. Machmoum, F. Poitiers, **"Sliding mode control of a variable speed wind energy conversion system with DFIG",** *International Conference and Exhibition on Ecologic Vehicles and Renewable Energies*, Monaco, 2009.

[6]. T. Noguchi, H. Tomiki, S. Kondo and I. Takahashi, **"Direct power control of PWM converter without power-source voltage sensors",** *IEEE Trans. Ind. Appl*, Vol. 34, 3, pp. 473–479, May–Jun. 1998.

[7]. M. Malinowski, M. P. Kazmierkowski, S. Hansen, F. Blaabjerg and G. D. Marques, **"Virtual-flux-based direct power control of three-phase PWM rectifiers",** *IEEE Trans. Ind. Appl*, Vol. 37, 4, pp. 1019–1027, Jul.–Aug. 2001.

[8]. A. Hossain Mollah, Prof. G K Panda, Prof. P K Saha, **"Three Phase Grid Connected Photovoltaic System with Maximum Power Point Tracking",** *IJAREEIE*, Vol. 4, Issue 5, pp. 2278-8875, May 2015.

[9]. Bimal K. Bose, **"Power Electronics and Motor Drives Advances and Trends",** *British Library Cataloguing-in-Publication Data*, London, 2006, pp. 209–217

[10]. T. Noguchi, H. Tomiki, S. Kondo and I. Takahashi, **"Direct Power Control of PWM Converter without Power- Source Voltage Sensors",** *IEEE Trans. Ind. Applicat.*, Vol. 34, 3, pp. 473-479, May/June, 1998.

[11]. Li ning, H.jingjing, Z.hui, W.yue, W.zhao'an, **"A novel direct power control strategy of three-level NPC rectifier without abnormal instantaneous reactive power fluctuation"**, *9th International Conference on Power Electronics-ECCE Asia*, Seoul, Korea. June 1-5, 2015

[12]. M.V. Kazemi, M. Moradi, R.V. Kazemi, **"Minimization of powers ripple of direct power controlled DFIG by fuzzy controller and improved discrete space vector modulation",** *Electric Power Systems Research,* Vol. 89, pp. 23–30, 2012

[13]. A. julean, **"Aactive damping of LCL filter resonance in grid connected applications"**, *Master Thesis*, PED10-1035 - Spring Semester, 2009.

[14]. Hornik, M. Stinchcombe and H. White, **"Multilayer feed forward networks are universal approximators",** *Neural Networks 1989*, Vol. 2, pp. 359-366

[15]. P. Werbos, **"Beyond regression: new tools for prediction and analysis in the behavioral sciences",** *PhD thesis, Cambridge*, MA: Harvard University Committee on Applied Mathematics, 1974.

[16]. D. Kukolj, F. Kulic and E. Levi. **"Design of Speed Controller for Sensorless Electric Drives based on AI Techniques: a comparative study",** *Artificial Intelligence in Engineering,* Vol. 14, pp. 165- 174, 2000.

[17]. R. Kumar, R. A. Gupta, S.V. Bhangale, and H. Gothwal. **"Artificial neural network based direct torque control of induction motor drives"**, *IETECH Journal of Electrical Analysis*, Vol. 2, pp. 159-165, 2008.

[18]. Cirrincione, M.C. Lu, and M. Pucci, **"Direct torque control of induction motors by use of the GMR neural network",** *International Joint Conference on Neural Networks*; 20-24 July 2003. Portland, Oregon, USA. pp. 2106-2111.